A search for factors influencing etioplast–chloroplast transition

Birgit Pudelski[a,b], Jürgen Soll[a,b], and Katrin Philippar[a,b,1]

[a]Biochemie und Physiologie der Pflanzen, Department Biologie I—Botanik, Ludwig-Maximilians-Universität München, Grosshadernerstrasse 2-4, D-82152 Planegg-Martinsried, Germany; and [b]Munich Center for Integrated Protein Science, Ludwig-Maximilians-Universität München, Feodor-Lynen-Strasse 25, D-81377 Munich, Germany

Edited by Bob B. Buchanan, University of California, Berkeley, CA, and approved May 26, 2009 (received for review February 26, 2009)

Chloroplast biogenesis in angiosperm plants requires the light-dependent transition from an etioplast stage. A key factor in this process is NADPH:protochlorophyllide oxidoreductase A (PORA), which catalyzes the light-dependent reduction of protochlorophyllide to chlorophyllide. In a recent study the chloroplast outer envelope channel OEP16 was described to be involved in etioplast to chloroplast transition by forming the translocation pore for the precursor protein of PORA [Pollmann et al. (2007) *Proc Natl Acad Sci USA* 104:2019–2023]. This hypothesis was based on the finding that a single *OEP16.1* knockout mutant in *Arabidopsis thaliana* was severely affected during seedling de-etiolation and PORA protein was absent in etioplasts. In contrast, in our study the identical T-DNA insertion line greened normally and showed normal etioplast to chloroplast transition, and mature PORA was present in etioplasts [Philippar et al. (2007) *Proc Natl Acad Sci USA* 104:678–683]. To address these conflicting results regarding the function of OEP16.1 for PORA import, we analyzed several lines segregating from the original *OEP16.1* T-DNA insertion line. Thereby we can unequivocally show that the loss of OEP16.1 neither correlates with impaired PORA import nor causes the observed de-etiolation phenotype. Furthermore, we found that the mutant line contains at least 2 additional T-DNA insertions in the genes for the extracellular polygalacturonase converter *AroGP1* and the plastid-localized chorismate mutase *CM1*. However, detailed examination of the de-etiolation phenotype and a genomewide transcriptional analysis revealed no direct influence of these genes on etioplast to chloroplast transition in *Arabidopsis* cotyledons.

chloroplast biogenesis | chloroplast outer envelope channel OEP16 | NADPH:protochlorophyllide oxidoreductase | protein import | solute transport

Chloroplasts, which originated from the endosymbiosis of an ancestor of today's cyanobacteria with a mitochondria-containing host cell (1), are the site of photosynthesis and thus represent the basis for all life dependent on atmospheric oxygen and carbohydrate supply. In higher plants, however, other types and more diverse functions of the plastid organelle family exist. Chloroplasts and nonphotosynthetic plastids of roots, pollen, and embryos provide essential compounds such as carbohydrates, amino acids, fatty acids, or secondary metabolites for plant growth and development. During biogenesis proplastids in meristematic tissue and etioplasts in dark-grown plantlets develop into the mature, photosynthetic chloroplast of the green leaf (2). As their Gram-negative bacterial ancestors, all plastids are enclosed by 2 membranes, the outer and inner envelopes, which in addition to many biosynthetic capacities have to fulfill 2 distinct transport functions: (*i*) Because of their biosynthetic activity plastids are closely linked to the metabolic network of the plant cell. Thus, both envelope membranes mediate metabolite and solute exchange via specific channels and transporters (3, 4). (*ii*) In the course of organelle evolution, most of the endosymbiont's genes were transferred to the host nucleus (5, 6) and therefore plastids have to import the vast majority of their protein constituents as precursors in a posttranslational event from the cytosol. In consequence the outer and inner envelope membranes are equipped with abundant protein translocon complexes (7–9).

In general, preproteins imported into chloroplasts contain an N-terminal transit peptide that is both necessary and sufficient for targeting and translocation. Upon translocation, the transit peptide is cleaved off by a stromal processing peptidase and the mature protein is formed (10). For most preproteins containing a cleavable N-terminal transit peptide, recognition and translocation are achieved by 2 distinct translocon complexes: the translocon of the outer envelope membrane of chloroplasts (TOC) and the translocon of the inner envelope membrane of chloroplasts (TIC), situated in the outer and the inner envelope membranes, respectively. The TOC complex is composed of 3 core subunits, i.e., the GTP-dependent TOC33/TOC34 receptors, the GTP-dependent TOC159 precursor binding and motor protein, and the TOC75 translocation channel (11, 12). In addition to this classical transit peptide-mediated protein translocation, several findings suggest that further import pathways exist. Proteins like a quinone oxidoreductase homolog (ceQORH, refs. 13 and 14), TIC32 (15), and further integral proteins in the inner envelope membrane of chloroplasts (16) are imported without a cleavable presequence, but targeting is provided by internal sequence information. Except for TOC75 all membrane proteins in the outer envelope known so far are targeted to plastids without a classical transit peptide (17).

Although it possesses an N-terminal transit peptide, an even more complex import pathway has been proposed for the preprotein of the plastid localized enzyme NADPH:protochlorophyllide oxidoreductase (POR, refs. 18–27). POR catalyzes the light-dependent conversion of protochlorophyllide (Pchlide) to chlorophyllide (Chlide), which represents a central reaction in chlorophyll biosynthesis and thus plastid differentiation in angiosperms (28, 29). In the model plant *Arabidopsis* 3 POR isoforms exist: PORA, -B, and -C (30). Early in seedling development the PORA and PORB genes are strongly expressed. However, PORA is present only in etiolated tissue in the dark but is rapidly degraded in the light. In etioplasts of angiosperms, which contain a large prolamellar body and prothylakoids instead of thylakoids (31), the prolamellar body consists to a large extent of the Pchlide holochrome, comprising PORA, its substrate Pchlide, and NADPH (32). Thus, PORA is responsible for Pchlide conversion upon illumination of seedlings catalyzing the essential light-dependent step in the etioplast to chloroplast transition during greening (de-etiolation). In contrast, PORB, which is stable in the light and regulated in a circadian rhythm (30, 33), and PORC, which is present in the leaves of light-grown plants (34), display expression patterns reflecting their function in constitutive chlorophyll biosynthesis (35). Whereas the preprotein prePORB seems to follow the general TOC-TIC import

Author contributions: J.S. and K.P. designed research; B.P. performed research; B.P. and K.P. analyzed data; and J.S. and K.P. wrote the paper.

Conflict of interest: The authors declare no conflict of interest.

This article is a PNAS Direct Submission.

[1]To whom correspondence should be addressed. E-mail: philippar@lrz.uni-muenchen.de.

This article contains supporting information online at www.pnas.org/cgi/content/full/0902145106/DCSupplemental.

pathway, the import of prePORA was suggested to diverge at the outer envelope membrane. In vitro import of prePORA was described by Reinbothe and coworkers to depend strictly on its substrate Pchlide (18–21, 24, 27), thereby using a so-called Pchlide-dependent translocon complex. In vivo data, however, revealed that this pathway is organ specific because prePORA requires its substrate Pchlide only in cotyledons to become imported into etioplasts and chloroplasts (22, 23). The substrate dependence is lost in true leaves and therefore seems to be developmentally regulated in planta [for details see supporting information (*SI*) *Discussion*].

During in vitro import into isolated plastids from leaves of barley seedlings the outer envelope channel OEP16 was identified by Reinbothe and coworkers as a proteinaceous subunit of the Pchlide-dependent translocon complex by chemical cross-linking and co-immunoprecipitation of the PORA precursor (20, 21, 24). According to phenotype analysis of an *OEP16.1* knockout line in *Arabidopsis* it was then postulated that OEP16 represents the translocation pore for PORA (25). Originally OEP16 was isolated as a transmembrane-spanning protein of 16 kDa from the outer envelope membrane of pea chloroplasts (36). When reconstituted into lipid bilayer membranes, the corresponding recombinant Ps-OEP16 protein formed a slightly cation-selective channel with transport selectivity for amino acids and amines. Subsequent studies on the phylogeny and secondary structure revealed that OEP16 belongs to the superfamily of preprotein and amino acid transporters (PRAT) including the protein translocating channels Tim17, Tim22, and Tim23 of the inner mitochondrial membrane (16, 37). Like these transporters, OEP16 forms 4 α-helical transmembrane domains (38). In *Arabidopsis* 3 genes are coding for OEP16 isoforms, named OEP16.1, OEP16.2, and OEP16.4, respectively (16, 39). At-OEP16.2 is expressed exclusively in plastids of late embryo development, early cotyledons, and pollen grains, whereas low levels of At-OEP16.4 transcripts are ubiquitously present. At-OEP16.1 is the most prominent isoform in the outer envelope membrane of *Arabidopsis* leaf chloroplasts (16, 39–41) and shows the highest sequence identity with OEP16 from pea and barley. In a study on chloroplast biogenesis using a mutant approach with single- and double-knockout lines for all plastid-localized *Arabidopsis* OEP16 isoforms we could show that none of the OEP16 isoforms is involved in prePORA import into cotyledon chloroplasts and etioplasts in vitro and in vivo (39).

However, Reinbothe and coworkers came to a completely converse conclusion using an *OEP16.1* single-knockout line of the same origin (25). They report a strong de-etiolation phenotype during seedling growth of the T-DNA insertion line SALK_024018 (42). When seedlings were first grown in darkness and afterward exposed to white light, mutants rapidly bleached and died because of the phototoxic effect of free Pchlide *a*, which is not bound in the Pchlide holochrome and thus acts as a potent photosensitizer that upon illumination generates toxic singlet oxygen (43). Mutant plants grown under continuous white light, however, were of wild-type appearance. This phenotype is well described for mutants of the *FLU* (*fluorescence*) gene in *Arabidopsis* (44, 45). Because FLU, a membrane-bound plastid protein, is a negative regulator of chlorophyll synthesis, conditional *flu* mutants accumulate free Pchlide in darkness. Immediately after a dark to light shift, *flu* seedlings bleach and die, whereas mature *flu* plants, which can survive the photooxidative stress caused by Pchlide, stop growing. In consequence, *flu* mutants have to be grown under continuous illumination, which inhibits accumulation of Pchlide because of its permanent light-dependent photoconversion. Because the T-DNA in SALK_024018 is causing a knockout of the gene *OEP16.1* and according to their previous in vitro studies (20, 21, 24), Reinbothe and coworkers conclude that OEP16.1 is the translocation pore for prePORA in the outer envelope membrane of plastids (25). Further, they postulate that the loss of OEP16.1 results in a lack of PORA in etioplasts that leads to the accumulation of free Pchlide *a* and in turn photo-oxidative damage of seedlings during dark to light transition. In contrast to the results of Reinbothe and coworkers, in our study the identical T-DNA insertion line for *OEP16.1* greened and developed normally under a day–night regime and showed wild-type etioplast to chloroplast transition (39).

Table 1. De-etiolation phenotype in the T-DNA insertion line SALK_024018

	oep16.1–1	det-p, %	*n*
Col-0	wt	14.7	265
flu	wt	31.6*	196
F6–4a	ho	70.7*	215
5.2	ho	85.8*	190
5.10	ho	49.2*	130
4.1	ho	15.0	233
4.2	wt	46.9*	177
19.3	wt	48.4*	182
2.2	wt	5.1	217

Except Col-0 and *flu*, all plants are progeny of the T-DNA insertion line SALK_024018 (see Fig. S2). F6–4a was published as *Atoep16–1* by Reinbothe and coworkers (25). The de-etiolation phenotype (det-p) was monitored in 3 independent experiments on seedlings grown for 2.5 days in darkness. Three days after transfer to continuous white light (350 μmol · m^{-2} · sec^{-1}), bleached, dead seedlings (compare Fig. 1) were quantified in percentage of all plantlets. wt, wild type for the *oep16.1–1* allele; ho, homozygous for *oep16.1–1*; *n*, number of seedlings monitored in at least 3 independent experiments. *, Lines with >30% dead seedlings (compare heterozygous *flu* control) were considered to show a de-etiolation phenotype. In parallel, all lines were PCR genotyped for the *oep16.1–1* T-DNA insertion.

Results

The Knockout of *OEP16.1* Is Not Linked to De-Etiolation. To evaluate the proposed function of OEP16.1 during seedling de-etiolation, we analyzed the phenotype described by Reinbothe and colleagues in several lines segregating from the original T-DNA insertion line SALK_024018. In this assay we first observed that the homozygous *oep16.1–1* line that had been used for all experiments in our previous study (39) did not show a de-etiolation phenotype. However, to our surprise line 3.1, representing the respective wild type for the *oep16.1–1* allele, displayed a phenotype in 37% of the seedlings tested. For quantification of the de-etiolation phenotype in 3 independent experiments we further included the homozygous *oep16.1–1* line F6–4a that was used in the study by Reinbothe and coworkers (25), direct progeny of freshly ordered SALK_024018 seeds, and as controls a heterozygous *flu* mutant (44) and Col-0 wild type (Table 1). In all lines tested, the de-etiolation phenotype was detectable in different quantities, ranging from 5 to 15% background of nongreening bleached seedlings in Col-0 wild-type and SALK_024018 lines 4.1 and 2.2 to severely affected in lines with 70–86% phenotype (F6–4a and 5.2). In parallel to phenotype quantification, PCR genotyping of all lines for the *oep16.1–1* mutant allele (Table 1) showed again that the de-etiolation phenotype was not segregating with the knockout of *OEP16.1*. We observed a phenotype in lines that were wild type for the *oep16.1–1* allele, e.g., lines 4.2 and 19.3. Vice versa, we identified lines homozygous for *oep16.1–1* without any de-etiolation defect, i.e., line 4.1. Furthermore, we monitored the accumulation of Pchlide in cotyledons of all lines tested by fluorescence microscopy (Fig. 1). While the Pchlide accumulation in the *flu* mutant led to a bright red fluorescence signal, the signal in lines F6–4a, 5.2, and 19.3 was less intense and of more orange color. The same fluorescence signal was detected in lines 4.2 and 5.10, which displayed the same quantity of phenotype as line 19.3 (compare with Table 1). In contrast, Col-0 wild type and lines without any de-etiolation defects (e.g., 4.1 and 2.2) showed yellow fluorescence. Furthermore, when grown under a normal day/night regime, all lines except *flu*, which stopped

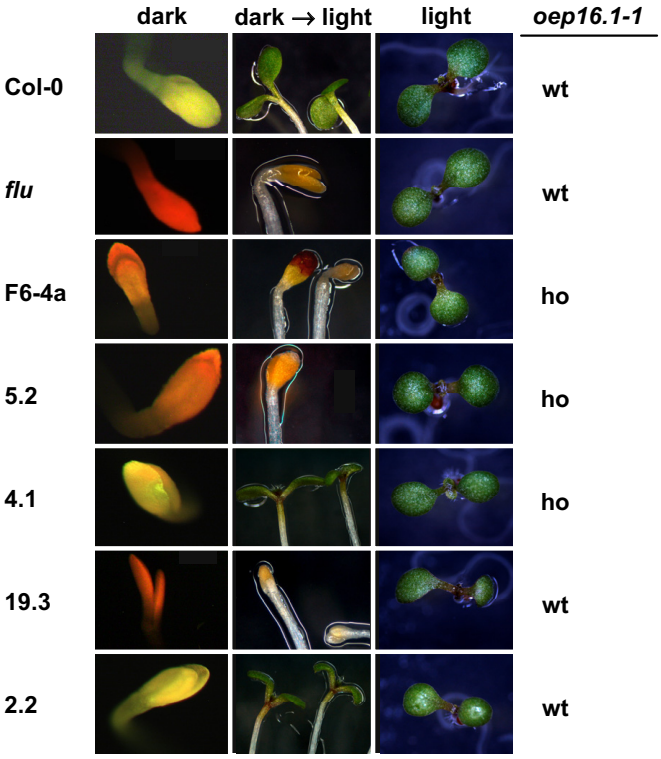

Fig. 1. De-etiolation phenotype in different lines of SALK_024018. All seedlings of different SALK_024018 lines (F6–4a, 5.2, 4.1, 19.3, and 2.2), Col-0 wild type, and *flu* mutants depicted display the representative appearance of 50 plantlets, analyzed in at least 3 independent experiments. The homozygous (ho) or the wild-type (wt) state of the *oep16.1–1* allele is indicated. (*Left*) After growth for 2.5 days in darkness, free Pchlide was monitored by fluorescence microscopy. Note that cotyledons that do not accumulate Pchlide show a yellow fluorescence (Col-0, 4.1, and 2.2), whereas free Pchlide is detected by a strong red fluorescence in *flu* mutants and a less intense orange signal in lines F6–4a, 5.2, and 19.3. (*Center*) De-etiolation was induced by a dark to light shift (350 μmol · m^{-2} · sec^{-1}). Three days after illumination, bleached seedlings were depicted in lines displaying a phenotype (*flu*, F6–4a, 5.2, and 19.3). (*Right*) For control, plantlets were grown under continuous light.

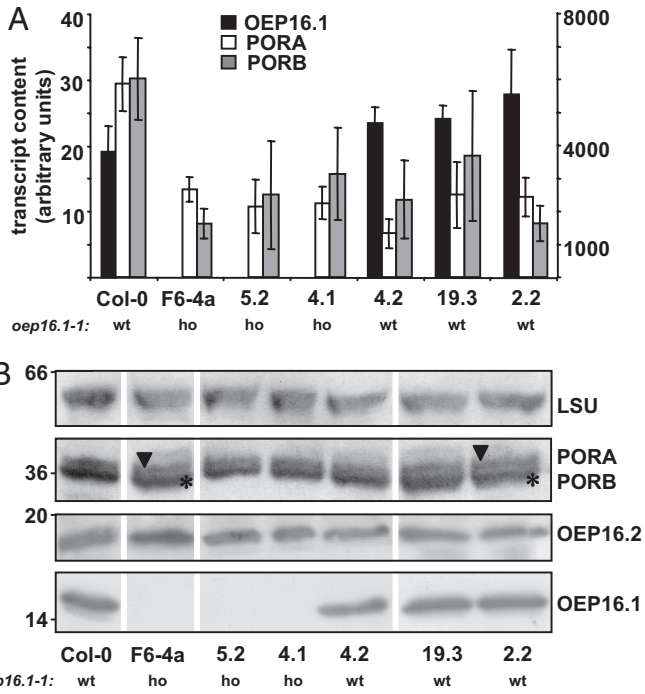

Fig. 2. Expression of OEP16.1, PORA, and PORB in etiolated cotyledons of different SALK_024018 lines. (*A*) Quantification of OEP16.1 (black), PORA (white), and PORB (gray) mRNA by quantitative real-time RT-PCR in 7-day-old etiolated cotyledons of Col-0 and different SALK_024018 lines (F6–4a, 5.2, 4.1, 4.2, 19.3, and 2.2). The homozygous (ho) or the wild-type (wt) state of the *oep16.1–1* allele is indicated. The transcript content ($n = 3 \pm$ SD, in arbitrary units) was quantified relative to the signal of 10,000 actin 2/8 molecules. Note that the *y* axis is divided into 2 different scales for OEP16.1 (left, 19–28 transcripts/10,000 actin 2/8 molecules) and PORA and PORB (right, 1321–6013 transcripts/10,000 actin 2/8 molecules). (*B*) Equal amounts of total protein (30 and 90–100 μg for detection of PORA/B and LSU, and OEP16.1 and OEP16.2 proteins, respectively) from plantlets in *A* were subjected to immunoblot analysis of OEP16.1, PORA, and PORB. Antisera against the large subunit of Rubisco (LSU) and OEP16.2 were used as controls. Numbers indicate the molecular mass of proteins in kilodaltons. Because the POR antibody used recognizes all isoforms, 2 bands, corresponding to the mature PORA (36.6 kDa, arrowhead) and PORB (36.4 kDa, asterisk) proteins, were detected in all plants analyzed.

growing as described in the literature (44), were of wild-type appearance. In summary, our phenotype analysis reveals that several lines of SALK_024018 display a de-etiolation defect. However, this phenotype is less strong than that reported by Reinbothe and coworkers and is not segregating with the knockout of *OEP16.1*.

Mature PORA and PORB Proteins Are Present in Etioplasts of *OEP16.1* Mutant Lines. In addition to the de-etiolation phenotype Reinbothe and colleagues described, PORA protein was reported to be lacking in etioplasts of the *oep16.1–1* mutant line. Thus, we compared PORA expression and the presence of mature PORA protein in etiolated seedlings of several lines, which where either homozygous or wild type for the *oep16.1–1* allele, by quantitative RT-PCR, immunoblot analysis, and mass spectrometry (Fig. 2, Fig. S1). As shown in Fig. 2*A*, neither the knockout of *OEP16.1* (lines F6–4a, 5.2, and 4.1) nor the presence of the de-etiolation phenotype (lines F6–4a, 5.2, 4.2, and 19.3) significantly affected the transcript content of PORA or PORB. In contrast to Reinbothe and coworkers (25) we detected mature PORA protein by immunoblot analysis in extracts from etiolated cotyledons of all lines analyzed (Fig. 2*B*). Because PORA and PORB, due to their high sequence similarity, cannot be unequivocally distinguished by immunoblot analysis, the protein band corresponding to mature POR (36 kDa) was excised from SDS gels and subjected to mass spectrometry. Again we were able to identify specific peptide fragments of PORA and PORB protein in etiolated cotyledons of all lines analyzed (Fig. S1, compare with ref. 39). Thus, we conclude that neither the lack of OEP16.1 nor the presence of the mild de-etiolation phenotype observed in the background of the SALK_024018 T-DNA line affect PORA and PORB expression in etiolated seedlings. We deduce that the import of prePORA and prePORB is not impaired in these plants.

The Mutant Line SALK_024018 Contains at Least 3 Different T-DNA Insertions. As described previously (39), the T-DNA insertion in *OEP16.1* in SALK_024018 is characterized by a concatemeric, back-to-back arrangement of pROK2 (Fig. 3*A*). Because several lines of SALK_024018, which were wild type for the *oep16.1–1* allele, displayed a mild de-etiolation defect, we analyzed whether additional T-DNA insertions might be present by screening for kanamycin resistance and PCR genotyping. All seedlings homozygous for *oep16.1–1* grew well on kanamycin, and on DNA of the same lines a 1209-bp PCR fragment was amplified by M13 primers, confirming the presence of the pROK2 T-DNA (42). However, lines 4.2 and 2.2, which were wild type for the *oep16.1–1* allele, also displayed 100% kanamycin resistance and M13-PCR products, indicating the presence of >1 T-DNA. To track these additional insertions, we performed several rounds of inverse PCR and

PLANT BIOLOGY

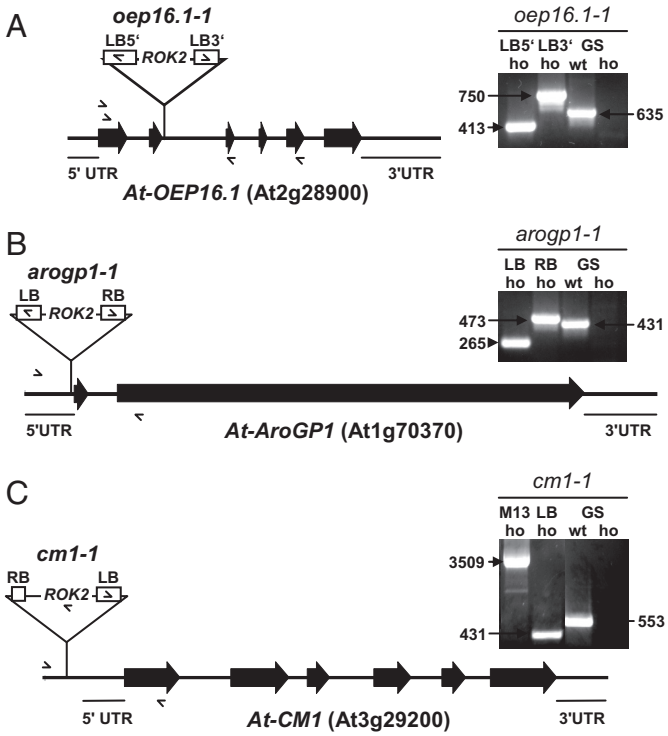

Fig. 3. Molecular characterization of T-DNA insertions in SALK_024018. Insertion sites and segregation of all identified T-DNAs in SALK_024018 were characterized by PCR genotyping using gene- (GS) and T-DNA-specific (LB, RB) primer combinations. Exons are depicted as solid bars, intron regions as solid lines, and positions for oligonucleotide primers are indicated by arrows. (*A*) In *OEP16.1* pROK2 inserts 8 bp before the 3′ end of exon 2, interrupting the ORF after amino acid 52. Note that at least 2 T-DNA molecules inserted back-to-back, forming a concatemer with the left border sequence at the 5′ and 3′ ends of the *OEP16.1*/T-DNA borders (LB5′ and LB3′). (*Right*) In homozygous *oep16.1–1* mutants gene-specific sense and antisense primers in combination with the left border primer amplify products of 413 and 750 bp, respectively (LB5′, LB3′). In lines wild type for the *oep16.1–1* allele a 635-bp PCR product is detected by a gene-specific primer pair, whereas the same product is absent in homozygous *oep16.1–1* (GS wt, GS ho). (*B*) The T-DNA pROK2 was detected in the 5′-UTR, 4 bp upstream of the start codon of the polygalacturonase converter gene *AroGP1*. Here the left border of pROK2 is oriented in the 5′ direction while in 3′ the right border is flanking *AroGP1*. At the insertion site the T-DNA causes a 13-bp deletion. (*Right*) Gene-specific sense and antisense primers in combination with LB and RB primers amplify products of 265 and 473 bp on DNA of homozygous *arogp1–1* mutants. Homozygosity of *arogp1–1* lines is proved by the absence of a 431-bp PCR product, amplified by the gene-specific primers on wild-type *AroGP1* (GS wt, GS ho). (*C*) The third T-DNA present in SALK_024018 inserts into the promoter region, 221 bp upstream of the translation start of chorismate mutase 1 (*CM1*). At the 5′ end of the T-DNA a truncated right border is flanking the *CM1* gene, while the left border is located at the 3′ end. Further, the insertion leads to a deletion of 179 bp. (*Right*) In homozygous *cm1–1* mutants gene-specific sense and antisense primers in combination with an internal T-DNA primer (truncated RB) and the left border primer amplify products of 3,509 and 431 bp, respectively. In lines wild type for *cm1–1* a 553-bp PCR product is detected by the gene-specific primer pair, whereas the same product is absent in homozygous *cm1–1* (GS wt, GS ho).

thermal asymmetric interlaced (TAIL)-PCR reactions on DNA isolated from different lines segregating from SALK_024018 (for details see *SI Methods* and Table S1).

In line 3.1, which is wild type for the *oep16.1–1* allele and segregated in parallel to the *oep16.1–1* mutant described in our previous study (ref. 39; see Fig. S2), we were able to identify a second T-DNA insertion by inverse PCR (Fig. 3*B*). Here pROK2 inserted in the 5′-UTR, 4 bp upstream of the coding region for At1g70370, which is highly similar to AroGP1, the noncatalytic β subunit of the polygalacturonase isozyme 1 (PG1) from tomato.

Table 2. T-DNA insertions and de-etiolation phenotype in different lines of SALK_024018

	oep16.1–1	*arogp1–1*	*cm1–1*	det-p, %	*n*
Col-0	wt	wt	wt	14.7	265
flu	wt	wt	wt	31.6*	196
F6–4a	ho	wt	wt	70.7*	215
5.2	ho	ho	ho	85.8*	190
5.10	ho	ho	ho	49.2*	130
4.1	ho	ho	wt	15.0	233
4.2	wt	ho	wt	46.9*	177
19.3	wt	wt	wt	48.4*	182
2.2	wt	wt	ho	5.1	217

Different lines segregating from SALK_024018, which displayed variable quantities of a de-etiolation phenotype (det-p) as described in Table 1, were PCR genotyped for the T-DNA insertions in *OEP16.1*, *AroGP1*, and *CM1*. wt, wild type; ho, homozygous for the respective mutant allele. *, Lines with >30% dead seedlings (compare heterozygous *flu* control) were considered to show a de-etiolation phenotype.

PG1 is a heterodimer built by AroGP1, also known as polygalacturonase converter, and PG2, the catalytic polygalacturonase subunit (46, 47). Thus, AroGP1, which is secreted to the apoplast, plays a role in regulating pectin metabolism during fruit ripening of tomato by limiting the pectin solubilization and depolymerization catalyzed by the action of the monomeric PG2 polygalacturonase. The 3 tomato isoforms AroGP1, -2, and -3 are similar to their *Arabidopsis* orthologs At1g70370, At1g23760, and At1g60390. Because At1g70370 displayed the highest similarity to AroGP1 (57% amino acid identity), in the following we refer to this protein as At-AroGP1 and to the T-DNA insertion mutant discovered in SALK_024018 as *arogp1–1* (Fig. 3*B*). So far, however, neither the proposed function of At-AroGP1 nor a phenotype of an *Arabidopsis* mutant line associated with the loss of At-AroGP1 have been published.

To our surprise we were able to identify a third T-DNA insertion in SALK_024018 by TAIL-PCR on DNA of line 2.2, which is wild type for the *oep16.1–1* and *arogp1* alleles (Fig. 3*C*). This approach revealed that pROK2 inserted into the putative promoter region of At3g29200, coding for the plastid-localized chorismate mutase 1 (CM1) in *Arabidopsis* (48–50). Chorismate mutase is the first enzyme of the branch of the shikimate pathway, which leads to the biosynthesis of the aromatic amino acids phenylalanine and tyrosine. Thereby CM catalyzes the conversion of chorismate into prephenate. In *Arabidopsis* 3 isoforms of chorismate mutase exist. Whereas CM1 and CM3 are predicted to be plastid localized, CM2 appears to be cytosolic (49, 50). Although the function of CM has been characterized in vitro in detail, nothing is known about the impact of plastid or cytosolic CM function in planta and no CM mutant lines have been described in *Arabidopsis* so far.

A Search for Factors Influencing Etioplast–Chloroplast Transition. To evaluate whether the identified mutations in *AroGP1* or *CM1* contribute to the de-etiolation phenotype detected in SALK_024018, we PCR genotyped all lines used in the phenotype analysis for the *aropg1–1* and *cm1–1* alleles. As shown in Table 2, however, neither homozygosity of *aropg1–1* nor homozygosity of *cm1–1* directly segregated with the de-etiolation phenotype. Whereas line 4.1 (homozygous for *oep16.1–1* and *aropg1–1*) displayed no de-etiolation defect, 46.9% of the seedlings from line 4.2, which proved to be homozygous for *aropg1–1*, showed damage during greening. Instead, a line homozygous for *cm1–1* (2.2) was not affected. An additive effect of all 3 mutations in *OEP16.1*, *AroGP1*, and *CM1* can be excluded as well (compare lines F6–4a, 5.2, 5.10, and 19.3 in Table 2). Further, line 19.3, which is wild type for all T-DNA insertions identified, showed impaired greening (48.4% defects), indicating that the phenotype is neither linked to

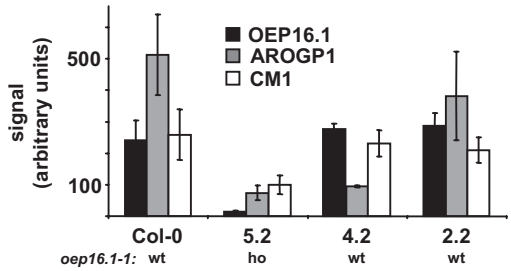

Fig. 4. Transcript levels of *OEP16.1*, *AroGP1*, and *CM1* in different SALK_024018 lines. Transcript content was determined by microarray analysis (Affymetrix ATH1 Genechip) in Col-0 wild type and SALK_024018 lines 5.2, 4.2, and 2.2. The homozygous (ho) or the wild-type (wt) state of the *oep16.1–1* allele is indicated. Microarray signals are made comparable by scaling the average overall signal intensity of all probe sets to a target signal of 100 (arbitrary units). The average (± SD) scaled signals of 3 independent experiments are shown ($n = 2$ for *AroGP1* in 4.2). Note that line 5.2 is homozygous for T-DNA insertions in *OEP16.1*, *AroGP1*, and *CM1*, while line 4.2 is homozygous for *arogp1–1* and line 2.2 for *cm1–1*, respectively. Whereas the T-DNA in *oep16.1–1* causes a knockout of *OEP16.1* in line 5.2, the insertions into the 5′-UTR of *AroGP1* and into the promoter region of *CM1* lead to a decrease of transcript content to 14.4% and 18.4% (*AroGp1* in 5.2 and 4.2) and 19.4% (*CM1* in 5.2) when compared to Col-0 signals. Although line 2.2 is homozygous for *cm1–1*, there is no significant reduction of mRNA when compared to wild-type lines (Col-0 and 4.2).

mutation of OEP16.1 nor coupled to mutation of AroGP1 or CM1. Because line 19.3 was not resistant to kanamycin and the M13-PCR proofing insertion of pROK2 failed, the de-etiolation phenotype in SALK_024018 most likely is not caused via a fourth T-DNA insertion but maybe by a point or footprint mutation. To exclude that a point mutation within the *FLU* gene is generating the observed defects in etioplast–chloroplast transition (compare with ref. 44) we cloned and sequenced >10 different PCR products of the *FLU* gene on genomic DNA of lines F6–4a and 19.3. However, no point or footprint mutation responsible for the observed de-etiolation phenotype could be detected within *FLU*.

To further identify genes with a function in etioplast–chloroplast transition, we performed DNA microarray analysis and compared the transcript content in 8-day-old seedlings from line 5.2 (85.8% phenotype, see Table 2) with that of lines 4.2, 2.2, and Col-0 wild type (46.9, 5.1, and 14.7% phenotypes, respectively, see Table 2). In general, except for OEP16.1, AroGP1, and CM1 (Fig. 4), transcript regulation of other genes was of weak significance. However, we selected 11 genes that displayed a slight decrease in mRNA content in lines exhibiting a phenotype (5.2 and 4.2) when compared to nonphenotype controls (lines 2.2 and Col-0). Proteins encoded by these genes were either predicted to be plastid localized or associated with a function that might be involved in de-etiolation. However, none of the isolated genomic DNA of all 11 candidates contained an additional T-DNA within the coding region or displayed other abnormalities. In addition, the reduced transcript content of the selected genes did not correlate with the de-etiolation phenotype. Thus, we conclude that these candidates are not directly involved in etioplast to chloroplast transition. Surprisingly the microarray analysis revealed that, although lines 2.2 and 5.2 are both homozygous for the *cm1–1* T-DNA insertion, only in line 5.2 was the transcript content of *CM1* reduced when compared to wild type (see Table 2 and Fig. 4). Because line 2.2 never displayed a de-etiolation phenotype, while line 5.2 is severely affected, reduced *CM1* transcripts might be linked to the phenotype.

Discussion

OEP16 Is Not Involved in Etioplast to Chloroplast Transition. We reproduced and quantified the de-etiolation phenotype of the *Arabidopsis* T-DNA insertion line SALK_024018 as described by Reinbothe and coworkers (25). However, this phenotype is less strong than that reported and more importantly it is not segregating with the knockout of *OEP16.1* (Table 1, Fig. 1). One striking impairment of the phenotype analysis by the Reinbothe group is that neither was the respective wild-type background for OEP16.1 in SALK_024018 included nor could the phenotype be reproduced by an independent *OEP16.1* knock-out allele or be complemented by the reintroduction of functional OEP16.1 protein (see *SI Discussion*). Further, they published a qualitative phenotype analysis only, lacking a statistical evaluation (i.e., analysis of different lines in independent biological replications). When these standard requirements of adequate mutant and phenotype analysis are provided (see Table 1), it becomes evident that the loss of OEP16.1 function is not segregating with the de-etiolation phenotype observed. Together with our previous analyses on single and double mutants of all OEP16 isoforms in *Arabidopsis*, which include in vitro protein import, gene expression, and electron microscopy data (39), and the fact that also the *OEP16.1*/*OEP16.2*/*OEP16.4* triple knock-out grows and develops normally under a standard day/night regime, we conclude that none of the *Arabidopsis* OEP16 proteins is involved in etioplast to chloroplast transition.

OEP16.1 Is Not the Import Pore for prePORA. By using urea-denatured precursor proteins, Reinbothe and coworkers showed that prePORA is not imported into plastids of their *oep16.1–1* mutant (25). However, when in vitro protein import is performed with nondenatured precursors, PORA translocation in OEP16 mutants is not impaired (ref. 39, see *SI Discussion*). Further, Reinbothe and colleagues described that mature PORA is absent in etioplasts of *oep16.1–1* mutants. In contrast, in the current study we showed that in none of the 6 different SALK_024018 lines used the transcript content of PORA in etioplasts was significantly changed when compared to wild type (Fig. 2*A*). Further, mature protein and peptides of PORA were detected as well (Fig. 2*B*, Fig. S1). In summary, in all lines analyzed PORA expression did not change with respect to OEP16.1 mutation or with respect to the de-etiolation phenotype. Thus, we conclude that neither the lack of OEP16.1 nor the presence of the mild de-etiolation phenotype observed in the background of the SALK_024018 T-DNA line affects PORA expression in etiolated seedlings. We deduce that the import of prePORA is not impaired in these plants and that OEP16.1 does not represent the import pore for prePORA.

From a physiological point of view, several observations argue also against OEP16.1 function in prePORA translocation. First, gene expression patterns of OEP16.1 and PORA are completely opposite. Corresponding to its strictly light-dependent function converting Pchlide into Chlide, PORA transcripts and protein in *Arabidopsis* are present in etiolated tissue only and rapidly degrade upon illumination (30). OEP16.1 in contrast is the major OEP16 isoform in green rosette leaves and during seedling development is expressed in response to light stimulus (39). Thus, it is not very likely that OEP16.1 transports precursor proteins in organs and physiological conditions when its gene expression is low but its substrate gene expression is high. Second, an impaired protein import of prePORA to etioplasts should not necessarily cause accumulation of Pchlide, unless the feedback inhibition by FLU is not working. If mature PORA cannot bind its substrate in the Pchlide holochrome of the prolamellar body in etioplasts (32), we assume that increased FLU expression and/or activity would feedback inhibit Pchlide biosynthesis and thereby prevent Pchlide accumulation. This point, however, can be clarified only by studies on mutant plants with reduced or no PORA protein.

New Factors Influencing Etioplast to Chloroplast Transition in *Arabidopsis*? The T-DNA insertion line SALK_024018 displayed a mild de-etiolation phenotype and is characterized by the mutation of at least 3 genes: *At-OEP16.1*, *At-AroGP1*, and *At-CM1*. However, none of these mutants could be directly correlated with the observed

phenotype (Table 2). Thus, it seems that OEP16.1, AroGP1, and CM1 are not involved in etioplast to chloroplast transition in *Arabidopsis*. Instead the function of OEP16 recently was linked to amino acid transport in planta (51). In this study, the seed-specific overexpression of a plasma membrane-localized amino acid permease in pea led to increased amino acid supply and OEP16 transcripts in embryos. Together with the in vitro selectivity of Ps-OEP16 for amino acids (36), it thus seems very likely that OEP16 is involved in amino acid transport across the outer envelope membrane of plastids. AroGP1 is a polygalacturonase converter, which is secreted to the apoplast and plays a role in regulating pectin metabolism during fruit ripening of tomato (46, 47). Hence, in *Arabidopsis*, it is implausible that AroGP1 functions in plastid biogenesis. Chorismate mutase is catalyzing a necessary step in the biosynthesis of the aromatic amino acids phenylalanine and tyrosine. Because aromatic amino acids are not only essential protein components, but also crucial precursors for a number of secondary plant metabolites, the loss of CM function should cause severe defects or even lethality. The *Arabidopsis* isoform CM1 is predicted to be plastid localized (49, 50) and therefore might play a role in chloroplast biogenesis. The *cm1–1* T-DNA insertion identified in SALK_024018 leads to a 179-bp deletion in the putative promoter region. However, this did not necessarily reduce *CM1* mRNA in homozygous *cm1–1* lines. Whereas in line 5.2 the transcript level of *CM1* was reduced, it was not significantly decreased in line 2.2. Interestingly, line 5.2 was characterized by a strong de-etiolation phenotype, while line 2.2 displayed no defect upon dark to light transition. Thus, it is tempting to speculate that deregulation of CM1 expression has an indirect effect on light-induced chloroplast biogenesis in *Arabidopsis* cotyledons.

Materials and Methods

Plant Material. Experiments were performed on *Arabidopsis thaliana* (L.) Heynh. Columbia (cv. Col-0; Lehle Seeds) and the SALK_024018 T-DNA insertion line (42). The heterozygous *flu* mutant was a gift of Klaus Apel (Boyce Thompson Institute for Plant Research, Ithaca, NY). Except Col-0 and *flu*, all plants are progeny of SALK_024018 as depicted in Fig. S2. For a detailed description of plant growth conditions refer to *SI Methods*.

Gene Expression Analysis. Immunoblot, peptide mass fingerprints, and transcript quantification were performed as described previously (39). For details see *SI Methods*.

ACKNOWLEDGMENTS. We thank Julia Neumann for technical assistance and Ulrike Oster for microarray data analysis. For help and advice with inverse PCR and TAIL-PCR we thank Jörg Meurer (Ludwig-Maximilians-Universität München, Germany) and Michael Büttner (University Erlangen-Nürnberg, Germany). We are indebted to Diter von Wettstein (Washington State University, Pullman, WA) for seeds of the *oep16.1–1* line F6–4a. This work was supported by grants from the Deutsche Forschungsgemeinschaft (to J.S.).

1. Gould SB, Waller RF, McFadden GI (2008) Plastid evolution. *Annu Rev Plant Biol* 59:491–517.
2. Waters M, Pyke K (2005) In *Plastids*, ed Möller SG (Blackwell, Oxford), pp 30–59.
3. Weber APM, Schwacke R, Flügge UI (2005) Solute transporters of the plastid envelope membrane. *Annu Rev Plant Biol* 56:133–164.
4. Philippar K, Soll J (2007) In *Plant Solute Transport*, eds Yeo AR, Flowers TJ (Blackwell, Oxford), pp 133–192.
5. Martin W, et al. (2002) Evolutionary analysis of Arabidopsis, cyanobacterial, and chloroplast genomes reveals plastid phylogeny and thousands of cyanobacterial genes in the nucleus. *Proc Natl Acad Sci USA* 99:12246–12251.
6. Leister D (2003) Chloroplast research in the genomic age. *Trends Genet* 19:47–56.
7. Stengel A, Soll J, Bölter B (2007) Protein import into chloroplasts: New aspects of a well-known topic. *Biol Chem* 388:765–772.
8. Inaba T, Schnell DJ (2008) Protein trafficking to plastids: One theme, many variations. *Biochem J* 413:15–28.
9. Gross J, Bhattacharya D (2009) Revaluating the evolution of the Toc and Tic protein translocons. *Trends Plants Sci* 14:13–20.
10. Richter S, Lamppa GK (1998) A chloroplast processing enzyme functions as the general stromal processing peptidase. *Proc Natl Acad Sci USA* 95:7463–7468.
11. Soll J, Schleiff E (2004) Protein import into chloroplasts. *Nat Rev Mol Cell Biol* 5:198–208.
12. Bédard J, Jarvis P (2005) Recognition and envelope translocation of chloroplast preproteins. *J Exp Bot* 56:2287–2320.
13. Miras S, et al. (2002) Non-canonical transit peptide for import into the chloroplast. *J Biol Chem* 277:47770–47778.
14. Miras S, et al. (2007) Toc159- and Toc75-independent import of a transit sequence-less precursor into the inner envelope of chloroplasts. *J Biol Chem* 282:29482–29492.
15. Nada A, Soll J (2004) Inner envelope protein 32 is imported into chloroplasts by a novel pathway. *J Cell Sci* 117:3975–3982.
16. Murcha MW, et al. (2007) Characterisation of the preprotein and amino acids transporter gene family in Arabidopsis. *Plant Physiol* 134:199–212.
17. Hofmann NR, Theg SM (2005) Chloroplast outer membrane protein targeting and insertion. *Trends Plant Sci* 10:450–457.
18. Reinbothe C, Lebedev N, Apel K, Reinbothe S (1997) Regulation of chloroplast protein import through a protochlorophyllide-responsive transit peptide. *Proc Natl Acad Sci USA* 94:8890–8894.
19. Reinbothe S, Mache R, Reinbothe C (2000) A second, substrate-dependent site of protein import into chloroplasts. *Proc Natl Acad Sci USA* 97:9795–9800.
20. Reinbothe S, Quigley F, Springer A, Schemenewitz A, Reinbothe C (2004) The outer plastid envelope protein Oep16: Role as precursor translocase in import of protochlorophyllide oxidoreductase A. *Proc Natl Acad Sci USA* 101:2203–2208.
21. Reinbothe S, Quigley F, Gray J, Schemenewitz A, Reinbothe C (2004) Identification of plastid envelope proteins required for import of protochlorophyllide oxidoreductase A into the chloroplast of barley. *Proc Natl Acad Sci USA* 101:2197–2202.
22. Kim C, Apel K (2004) Substrate-dependent and organ-specific chloroplast protein import in planta. *Plant Cell* 16:88–98.
23. Kim C, Ham H, Apel K (2005) Multiplicity of different cell- and organ-specific import routes for the NADPH-protochlorophyllide oxidoreductases A and B in plastids of Arabidopsis seedlings. *Plant J* 42:329–340.
24. Reinbothe S, et al. (2005) A role of Toc33 in the protochlorophyllide-dependent plastid import pathway of NADPH:protochlorophyllide oxidoreductase (POR)A. *Plant J* 42:1–12.
25. Pollmann S, et al. (2007) A plant porphyria related to defects in plastid import of protochlorophyllide oxidoreductase A. *Proc Natl Acad Sci USA* 104:2019–2023.
26. Schemenewitz A, Pollmann S, Reinbothe C, Reinbothe S (2007) A substrate-independent, 14:3:3 protein-mediated plastid import pathway of NADPH:protochlorophyllide oxidoreductase A. *Proc Natl Acad Sci USA* 104:8538–8543.
27. Reinbothe C, et al. (2008) A pentapeptide motif related to a pigment binding site in the major light-harvesting protein of photosystem II, LHCII, governs substrate-dependent plastid import of NADPH:protochlorophyllide oxidoreductase A. *Plant Physiol* 148:694–703.
28. Griffiths WT (1978) Reconstitution of chlorophyllide formation by isolated etioplast membranes. *Biochem J* 174:681–692.
29. Apel K, Santel HJ, Redlinger TE, Falk H (1980) The protochlorophyllide holochrome of barley (Hordeum vulgare L.). Isolation and characterization of the NADPH:protochlorophyllide oxidoreductase. *FEBS J* 111:251–258.
30. Su Q, Frick G, Armstrong G, Apel K (2001) POR C of Arabidopsis thaliana: A third light- and NADPH-dependent protochlorophyllide oxidoreductase that is differentially regulated by light. *Plant Mol Biol* 47:805–813.
31. Gunning BE (2001) Membrane geometry of ''open'' prolamellar bodies. *Protoplasma* 215:4–15.
32. Santel HJ, Apel K (1981) The protochlorophyllide holochrome of barley (Hordeum vulgare L.). The effect of light on the NADPH:protochlorophyllide oxidoreductase. *FEBS J* 120:95–103.
33. Armstrong GA, Runge S, Frick G, Sperling U, Apel K (1995) Identification of NADPH:protochlorophyllide oxidoreductases A and B: A branched pathway for light-dependent chlorophyll biosynthesis in Arabidopsis thaliana. *Plant Physiol* 108:1505–1517.
34. Oosawa N, et al. (2000) Identification and light-induced expression of a novel gene of NADPH-protochlorophyllide oxidoreductase isoform in Arabidopsis thaliana. *FEBS Lett* 474:133–136.
35. Frick G, Su Q, Apel K, Armstrong GA (2003) An Arabidopsis porB porC double mutant lacking light-dependent NADPH:protochlorophyllide oxidoreductases B and C is highly chlorophyll-deficient and developmentally arrested. *Plant J* 35:141–153.
36. Pohlmeyer K, Soll J, Steinkamp T, Hinnah S, Wagner R (1997) Isolation and characterization of an amino acid-selective channel protein present in the chloroplastic outer envelope membrane. *Proc Natl Acad Sci USA* 94:9504–9509.
37. Rassow J, Dekker PJ, van Wilpe S, Meijer M, Soll J (1999) The preprotein translocase of the mitochondrial inner membrane: Function and evolution. *J Mol Biol* 286:105–120.
38. Linke D, et al. (2004) Folding kinetics and structure of OEP16. *Biophys J* 86:1479–1487.
39. Philippar K, et al. (2007) Chloroplast biogenesis: The use of mutants to study the etioplast-chloroplast transition. *Proc Natl Acad Sci USA* 104:678–683.
40. Ferro M, et al. (2003) Proteomics of the chloroplast envelope membranes from *Arabidopsis thaliana*. *Mol Cell Proteomics* 2.5:325–345.
41. Kleffmann T, et al. (2004) The Arabidopsis thaliana chloroplast proteome reveals pathway abundance and novel protein functions. *Curr Biol* 14:354–362.
42. Alonso JM, et al. (2003) Genome-wide insertional mutagenesis of *Arabidopsis thaliana*. *Science* 301:653–657.
43. Runge S, Sperling U, Frick G, Apel K, Armstrong GA (1996) Distinct roles for light-dependent NADPH:protochlorophyllide oxidoreductases (POR) A and B during greening in higher plants. *Plant J* 9:513–523.
44. Meskauskiene R, et al. (2001) FLU: A negative regulator of chlorophyll biosynthesis in *Arabidopsis thaliana*. *Proc Natl Acad Sci USA* 98:12826–12831.
45. op den Camp RGL, et al. (2003) Rapid induction of distinct stress responses after the release of singlet oxygen in Arabidopsis. *Plant Cell* 15:2320–2332.
46. Moore T, Bennett AB (1994) Tomato fruit polygalacturonase isozyme 1 (characterization of the β subunit and its state of assembly in vivo). *Plant Physiol* 106:1461–1469.
47. Watson CF, Zheng L, DellaPenna D (1994) Reduction of tomato polygalacturonase β subunit expression affects pectin solubilization and degradation during fruit ripening. *Plant Cell* 6:1623–1634.
48. Eberhard J, Raesecke HR, Schmid J, Amrhein N (1993) Cloning and expression in yeast of a higher plant chorismate mutase. *FEBS Lett* 334:233–236.
49. Eberhard J, et al. (1996) Cytosolic and plastidic chorismate mutase isozymes from Arabidopsis thaliana: Molecular characterization and enzymatic properties. *Plant J* 10:815–821.
50. Mobley EM, Kunkel BN, Keith B (1999) Identification, characterization and comparative analysis of a novel chorismate mutase gene in Arabidopsis thaliana. *Gene* 240:115–123.
51. Weigelt K, et al. (2008) Increasing amino acid supply in pea embryos reveals specific interactions of N and C metabolism, and highlights the importance of mitochondrial metabolism. *Plant J* 55:909–926.